NATIONAL ADVISORY COMMITTEE FOR AERONAUTICS

TECHNICAL NOTE 2823

LANGLEY FULL-SCALE-TUNNEL INVESTIGATION OF THE MAXIMUM-LIFT AND STALLING CHARACTERISTICS OF A TRAPEZOIDAL WING OF ASPECT RATIO 4 WITH CIRCULAR-ARC AIRFOIL SECTIONS

By Roy H. Lange

Langley Aeronautical Laboratory
Langley Field, Va.

Washington
November 1952

1T

NATIONAL ADVISORY COMMITTEE FOR AERONAUTICS

TECHNICAL NOTE 2823

LANGLEY FULL-SCALE-TUNNEL INVESTIGATION OF THE MAXIMUM-LIFT AND STALLING CHARACTERISTICS OF A TRAPEZOIDAL WING OF ASPECT RATIO 4 WITH CIRCULAR-ARC AIRFOIL SECTIONS[1]

By Roy H. Lange

SUMMARY

The results of an investigation at high Reynolds numbers and low Mach numbers to determine the maximum-lift and stalling characteristics of an aspect-ratio-4 trapezoidal wing with 10-percent-thick, circular-arc airfoil sections are presented in this paper. The tests included measurements of the lift, the drag, and the pitching-moment coefficients of the basic wing and of the wing with 0.20-chord droop-nose and rear flaps deflected both alone and in combination with one another. Scale effects were investigated at Reynolds numbers ranging from 3.27×10^6 to 7.67×10^6. In addition to the force measurements, the stalling characteristics of the wing were determined by means of tuft observations.

The maximum lift coefficient of the basic wing is 0.63, and a value of 1.39 was obtained for the wing with the best combination of deflections of the droop-nose flaps and the full-span rear flaps. A droop-nose-flap deflection of 20° appears optimum for maximum lift with rear flaps both neutral and deflected 60°. The drag of the wing is high throughout the moderate and high angle-of-attack range. Deflecting the droop-nose flaps is effective in causing an appreciable reduction in the drag throughout the moderate and high angle-of-attack range. In general, the pitching-moment characteristics of the basic wing and of the wing with all combinations of flap deflection indicate a forward location of the center of pressure with respect to the quarter chord up to about 0.80 of maximum lift. With further increases in lift coefficient, the center of pressure of the basic wing and of the wing with flaps deflected individually moves rearward and large amounts of longitudinal stability are

---

[1]Supersedes the recently declassified NACA RM L7H19, "Langley Full-Scale-Tunnel Investigation of the Maximum Lift and Stalling Characteristics of a Trapezoidal Wing of Aspect Ratio 4 With Circular-Arc Airfoil Sections" by Roy H. Lange, 1947.

indicated through the stall. For the wing with the flaps deflected in combination with one another, marginal stability is indicated at the stall. The lift, the drag, and the pitching-moment coefficients of the wing are unaffected by variation of the Reynolds number in the range investigated.

INTRODUCTION

The development of airplanes that will fly in the transonic and supersonic speed ranges has focused increasing attention upon the characteristics of wings having airfoil sections with sharp leading edges. As would be expected, the analysis of two-dimensional data at large scale and three-dimensional data at small scale has indicated that these wings will have inherently poor characteristics in the landing and take-off attitudes. In order to provide large-scale three-dimensional data on the characteristics at high angles of attack of wings having airfoil sections with sharp leading edges, an investigation was conducted in the Langley full-scale tunnel at high Reynolds numbers and low Mach numbers of several typical transonic and supersonic wing plan forms having 10-percent-thick, circular-arc airfoil sections. As a part of this study, an investigation has been conducted on a trapezoidal wing of aspect ratio 4. The plan form was obtained by cutting the rear portion of the tips from a rectangular plan form at an angle of 30° to the stream direction. (See fig. 1.) This configuration appears interesting for the completely supersonic range since theoretical calculations indicate that, for the wing at a Mach angle of 30° (or Mach number of 2), the wake has no influence on the lifting surface and the drag coefficient is no greater than that for the airfoil section in two-dimensional flow. (See refs. 1 and 2.)

The investigation included measurements at high Reynolds numbers and low Mach numbers of the lift, the drag, and the pitching-moment coefficients of the basic wing and of the wing with the 0.20-chord droop-nose flaps and the 0.20-chord rear flaps deflected both alone and in combination with one another. The scale effect on the aerodynamic characteristics was determined for a range of Reynolds numbers from 3.27×10^6 to 7.67×10^6. In addition to the force measurements, the stalling characteristics of the wing for various combinations of flap deflections were determined by means of tuft observations.

COEFFICIENTS AND SYMBOLS

The test data are presented as standard NACA coefficients of forces and moments. The data are referred to the wind axes.

C_L	lift coefficient, Lift/qS
C_D	drag coefficient, Drag/qS
$C_{m_{c/4}}$	pitching-moment coefficient about the quarter chord, $\frac{M_{c/4}}{qSc}$
α	angle of attack, deg
q	free-stream dynamic pressure, lb/sq ft
$M_{c/4}$	pitching moment about quarter chord; positive when it tends to increase the angle of attack, ft-lb
S	wing area, 232.0 sq ft
c	wing chord, 9.23 ft
R	Reynolds number, $\rho Vc/\mu$
V	free-stream velocity, fps
ρ	mass density of air, slugs/cu ft
μ	coefficient of viscosity, slugs/ft sec
δ_n	droop-nose-flap deflection, deg
δ_f	rear-flap deflection, deg
$C_{L_{max}}$	maximum lift coefficient
$\alpha_{C_{L_{max}}}$	angle of attack for maximum lift, deg

MODEL

The geometric characteristics of the wing and the arrangement of the high-lift devices are given in figures 1 and 2. Photographs of the wing mounted on the Langley full-scale-tunnel balance supports are given in figures 3 and 4. The wing has a symmetrical circular-arc section 10 percent thick, the ordinates of which may be found in reference 3. The wedge-shape tips employed on the wing are considered a possible supersonic tip configuration. The wing has no geometric dihedral or twist.

The wing construction consisted of a simple framework of $\frac{1}{4}$-inch steel channel spars covered with a $\frac{1}{4}$-inch skin of aluminum sheet rolled to the correct airfoil contour. The wing surfaces were about the equivalent in roughness to conventional thin dural sheet construction with dimpled skin and unfilled flush rivets. The wing construction was extremely rigid and no deflections of an appreciable magnitude occurred during the tests. The wing was provided with 0.20c droop-nose and rear flaps pivoted on piano hinges mounted flush with the lower wing surface. The flap configurations investigated were full-span droop-nose flaps and rear flaps which were full-span and 45 percent of the wing trailing-edge span. The wing was designed so that rear flap deflections up to 60° and droop-nose deflections up to 40° could be obtained. For the tests with the droop-nose or rear flaps deflected, the flap gap on the upper wing surface was sealed with a faired cover plate.

TESTS

All the tests were made through an angle-of-attack range from about -2° through the stall. The tests were made at a Reynolds number of about 4.76×10^6 except where noted. Measurements of the lift, the drag, and the pitching moment were made at increments of angle of attack of 2° except near maximum lift where the increments were 1°. In order to determine the scale effect on the aerodynamic characteristics of the basic wing, tests were made at various tunnel airspeeds to give a Reynolds number range from 3.27×10^6 to 7.67×10^6. The highest Mach number obtained in these tests was 0.13, corresponding to a Reynolds number of 7.67×10^6.

In order to determine the effects of flap deflection on the aerodynamic characteristics of the wing, tests were made with the droop-nose flap and with the rear flaps deflected alone and in combination with one another. Tests were made with the rear flaps deflected in 15° increments of δ_f up to 60° and with the droop-nose flaps deflected in 10° increments of δ_n up to 40°. In addition, tests were made with the droop-nose flaps deflected 36° inasmuch as two-dimensional tests (ref. 3) indicated this setting to be optimum for maximum lift. For the tests with the droop-nose flaps and rear flaps deflected simultaneously, the rear flaps were deflected 60° and the droop-nose-flap deflection was varied from 0° to 40°.

The stalling characteristics were determined by observing the action of wool tufts attached to the upper wing surface. These tuft studies

were made of the basic wing and of the wing with the droop-nose flaps and rear flaps deflected ($\delta_n = 36^\circ$, $\delta_f = 60^\circ$) alone and in combination with one another.

RESULTS AND DISCUSSION

The results have been corrected for the stream alinement, the blocking effects, the jet-boundary effects, and the tares caused by the wing supports.

The discussion of the test results has been grouped into three main sections. The first section presents results showing the scale effect on the aerodynamic characteristics of the basic wing with flaps neutral. (See fig. 5.) The second section gives the results showing the effect on the aerodynamic characteristics of deflecting the rear and droop-nose flaps individually (figs. 6 and 7, respectively). For convenience, summary curves of the effect of the flaps on the maximum lift coefficient and angle of attack for maximum lift are presented in figure 8. The third section gives the results of tests made with the droop-nose flaps and rear flaps deflected simultaneously. (See fig. 9.) The stalling characteristics of the wing with the flaps neutral and deflected are shown in figure 10 and are discussed in each of the main sections of the results and discussion. The power-off landing-approach speed characteristics of the wing are given in figure 11 in the form of lines for both constant gliding and sinking speeds for a wing loading of 40 pounds per square foot superimposed on the lift-drag polars of several wing-flap configurations.

Characteristics of the Basic Wing

Force measurements.- As shown in figure 5(a), the maximum lift coefficient of the basic wing is 0.63. This value of maximum lift coefficient is slightly lower than the value of 0.67 obtained in two-dimensional tests of the airfoil section (ref. 3). The influence of the low aspect ratio can be seen in the shape of the lift curves which are nonlinear and have well-rounded peaks. The lift-curve slope (measured at $C_L = 0.2$ to avoid the slight discontinuity at lower lift coefficients) is 0.057. Calculations based on the lift-curve slope of 0.090 obtained in two-dimensional flow indicate that the value of 0.057 obtained from the tests of the wing is about what would be expected when the aspect ratio is considered.

The variation of the pitching-moment coefficient with lift coefficient indicates a forward location of the center of pressure with respect

to the quarter chord up to about $C_L = 0.50$ $\left(\text{or } 0.80C_{L_{max}}\right)$ after which the center of pressure moves rearward with increase in lift coefficient showing large amounts of stability through the stall. (See fig. 5(b).) The drag coefficient of the wing is high at the moderate and high angles of attack as compared with the drag of wings with conventional, round-nose airfoil sections.

The results of figure 5 show no appreciable scale effect on the aerodynamic characteristics of the wing through the range of Reynolds numbers from 3.27×10^6 to 7.67×10^6 because of the effect of the sharp leading edge which fixes the point of initial local separation. This local separation is further discussed in the following section on stalling characteristics.

Stalling characteristics.- Tuft studies of the basic wing at the leading edge of the wing center section (fig. 10(a)) show early separation which spreads rapidly toward the tips up to an angle of attack of about 7°. At this angle of attack the flow over the wing resembles the flow over the airfoil section in two-dimensional flow where a bubble of separation at the nose of the airfoil followed by smooth flow has been observed at low angles of attack. With further increases in the angle of attack the wing exhibits the usual flow characteristics of a rectangular wing inasmuch as the center section stalls first and then the stalled area spreads toward the tips. This stall progression results from the higher effective angle of attack of the root sections caused by the induced flow.

Effect of Flap Deflection

Rear flaps.- Maximum lift coefficients of 0.94 and 1.16, respectively, were obtained for the wing with partial-span and full-span rear flaps deflected 60°. These values are 0.31 and 0.53 higher than that obtained for the basic wing. (See figs. 6 and 8.) Approximate calculations were made by use of the methods of reference 4 and the two-dimensional section data of reference 3 in order to determine the increments in lift coefficient due to rear flap deflection. The calculated and measured values were in fair agreement; thus, it was indicated that the sharp-leading-edge wing responds to the simple high-lift devices in a manner similar to that of conventional wings. The pitching-moment curves indicate the usual change in trim with flap deflection and, as compared with the basic wing, there is no appreciable change in the longitudinal stability. Tuft studies of the wing with the full-span rear flaps deflected 60° (fig. 10(b)) show the early leading-edge stalling and other characteristics that were typical of the basic wing.

The evaluation of the usable lift coefficients of the wing in terms of power-off landing-approach characteristics is made possible by use of figure 11. The increase in lift due to rear flap deflection is shown here to be offset in part by a large increase in drag with the result that the gliding and sinking speeds considerably exceeded the criterion set forth in reference 5 of a sinking speed not exceeding 25 feet per second at about $0.85C_{L_{max}}$.

Droop-nose flaps.- The maximum lift coefficient of the wing with the droop-nose flaps deflected 20° was 0.95. (See fig. 7.) This maximum lift coefficient was obtained by delaying the stalling to higher angles of attack as compared with the basic wing. From figure 8 it appears that this droop-nose-flap deflection is optimum for maximum lift. The increases in maximum lift coefficient and angle of attack for maximum lift with the droop-nose flaps deflected are caused primarily by the improved flow conditions at the leading edge when the leading edge is more nearly alined with the air stream at moderate and high angles of attack. This alinement of the leading edge tends to alleviate the negative pressure peaks that cause leading-edge separation. The absence of leading-edge separation is indicated in the tuft studies of the wing with the droop-nose flaps deflected. (See fig. 10(c).) The initial separation has been delayed to higher angles of attack and moved back to the region of the hinge line of the flap.

Deflecting the droop-nose flaps caused an appreciable reduction in the drag of the wing at moderate and high angles of attack. The 20° deflection shows the lowest drag; therefore, this deflection is about optimum both for maximum lift and low drag in the moderate angle-of-attack range. The beneficial effect of droop-nose-flap deflection on the drag results in lower sinking speeds as shown in figure 11. At $0.85C_{L_{max}}$ a gliding speed of 138 miles per hour is obtained for a sinking speed of 25 feet per second. It should be realized that the drags plotted in figure 11 are for the wing alone and the sinking speeds of the complete airplane would be somewhat greater. Power could be used for the landing approach and landing conditions to offset the high drags shown in figure 11, but this practice would lead to dangerous conditions for emergency landings with power off.

The pitching-moment curves (fig. 7) show no significant change in the longitudinal stability of the wing as compared with the basic wing. A smaller change in trim due to droop-nose-flap deflection is noted than was measured with the rear flaps deflected.

Combined Deflections of Flaps

In general, the effects of droop-nose-flap deflection on the aerodynamic characteristics of the wing with rear flaps deflected were the

same as were noted in the tests of the wing with the droop-nose flaps deflected alone. Peak values of maximum lift coefficient of 1.20 and 1.39 were obtained for $\delta_n = 20^\circ$ with partial-span and full-span rear flaps deflected 60°, respectively. (See figs. 9(a) and 9(b).) These values are 0.27 and 0.23, respectively, higher than the values obtained with the rear flaps deflected alone. The sharp break in the lift curves at the stall is in contrast to the well-rounded peaks obtained for the basic wing and the wing with the droop-nose and rear flaps deflected individually. As was the condition with the droop-nose flaps deflected alone, a droop-nose-flap deflection of 20° appears optimum for both maximum lift and low drag. The stalling characteristics of the wing with $\delta_n = 36^\circ$ and $\delta_f = 60^\circ$ (fig. 10(d)) show initial separation in the region of the hinge line of the droop-nose flaps, which was noted in the tuft studies of the wing with the droop-nose flaps deflected alone (fig. 10(c)).

The variations of the pitching-moment-coefficient curves with lift coefficient show no significant change as compared with the curves for the wing with the droop-nose flaps deflected alone except that the longitudinal stability at the stall is marginal. With full-span rear flaps deflected (fig. 9(b)) there is an unstable break at the stall as compared with partial-span rear flaps deflected (fig. 9(a)). This condition is not considered serious because of the gradual progress of the break with angle of attack and the small magnitude of the change in pitching moments involved.

Although the gliding speeds shown in figure 11 are the lowest obtainable, the sinking speeds are increased considerably by deflection of the rear flaps as compared with those obtained for the wing with droop-nose flaps deflected.

SUMMARY OF RESULTS

The results of an investigation at high Reynolds numbers and low Mach numbers in the Langley full-scale tunnel of the maximum-lift and stalling characteristics of an aspect-ratio-4 trapezoidal wing with circular-arc airfoil sections are summarized as follows:

1. The maximum lift coefficient of the basic wing is 0.63. A maximum lift coefficient of 1.39 was obtained with the best combination of deflections of the droop-nose flaps and the full-span rear flaps.

2. A droop-nose-flap deflection of 20° appears optimum for maximum lift with the rear flaps both neutral and deflected 60°.

3. The drag of the wing is high throughout the moderate and high angle-of-attack range. Deflecting the droop-nose flaps is effective in causing an appreciable reduction in the drag throughout the moderate and high angle-of-attack range.

4. In general, the pitching-moment characteristics of the basic wing and of the wing with all combinations of flaps indicate a forward location of the center of pressure with respect to the quarter chord up to about 0.80 of maximum lift coefficient. With further increases in lift coefficient, the center of pressure of the basic wing and of the wing with flaps deflected individually moves rearward and large amounts of longitudinal stability are indicated through the stall. For the wing with the flaps deflected in combination with one another, marginal stability is indicated at the stall with an unstable break at the stall being measured for the full-span flaps.

5. The lift, the drag, and the pitching-moment coefficients of the wing are unaffected by the variation of Reynolds number in the range from 3.27×10^6 to 7.67×10^6.

Langley Aeronautical Laboratory,
National Advisory Committee for Aeronautics,
Langley Field, Va., August 27, 1947.

REFERENCES

1. Schlichting, H.: Airfoil Theory at Supersonic Speed. NACA TM 897, 1939.

2. Jones, Robert T.: Wing Plan Forms for High-Speed Flight. NACA Rep. 863, 1947. (Supersedes NACA TN 1033.)

3. Underwood, William J., and Nuber, Robert J.: Two-Dimensional Wind-Tunnel Investigation at High Reynolds Numbers of Two Symmetrical Circular-Arc Airfoil Sections With High-Lift Devices. NACA RM L6K22, 1947.

4. Silverstein, Abe, and Katzoff, S.: Design Charts for Predicting Downwash Angles and Wake Characteristics Behind Plain and Flapped Wings. NACA Rep. 648, 1939.

5. Gustafson, F. B., and O'Sullivan, William J., Jr.: The Effect of High Wing Loading on Landing Technique and Distance, With Experimental Data for the B-26 Airplane. NACA ARR L4K07, 1945.

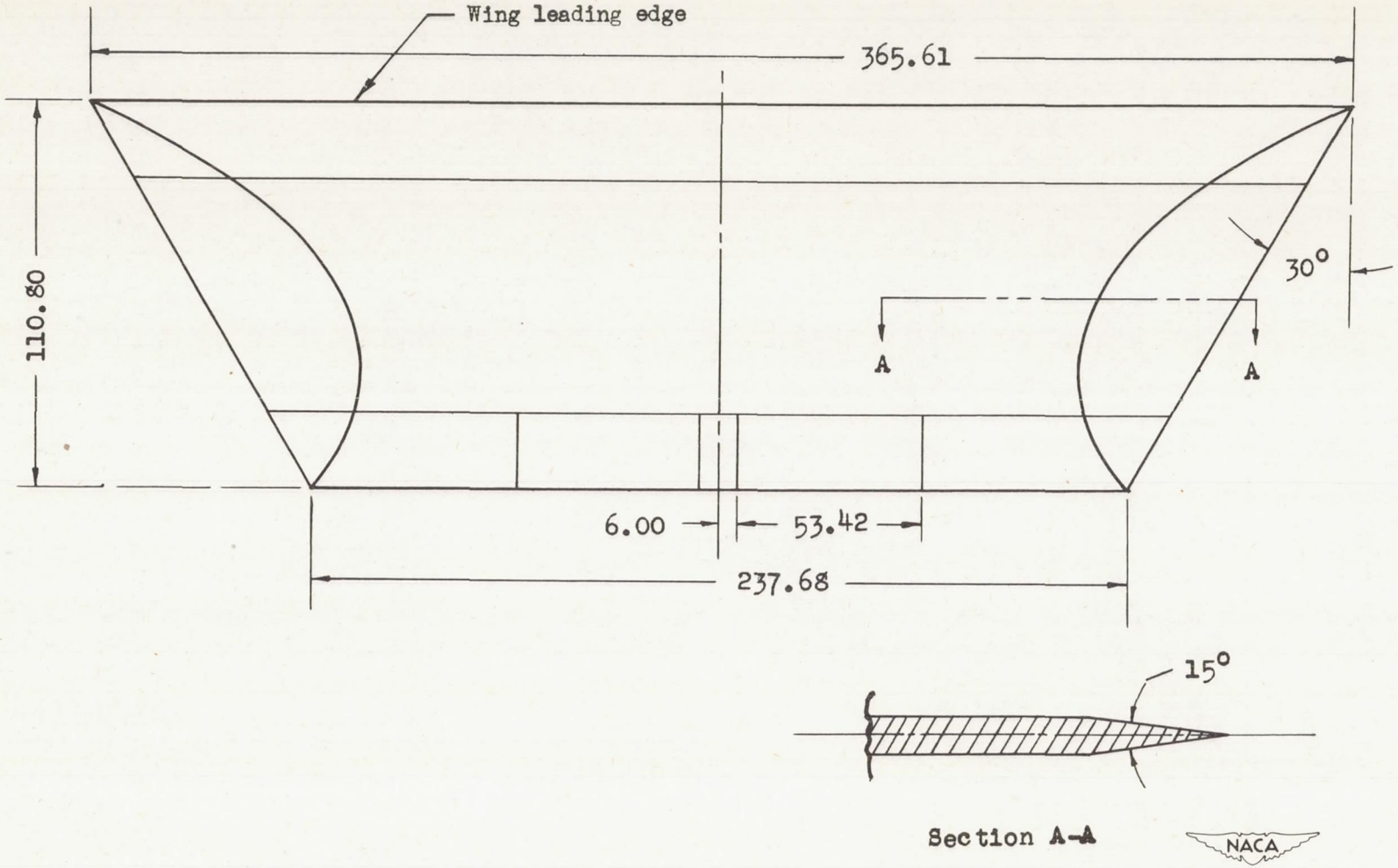

Figure 1.- Geometric characteristics of trapezoidal wing. Wing area, 232.0 square feet; aspect ratio, 4.0. All dimensions are given in inches.

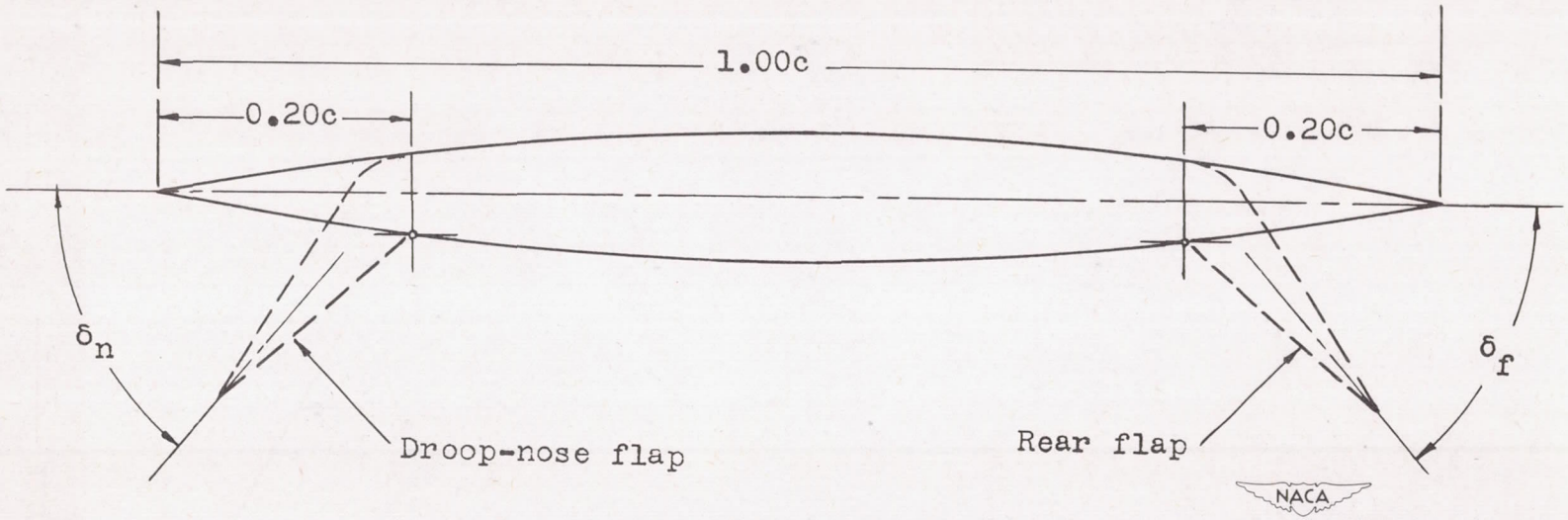

Figure 2.- Sketch of circular-arc airfoil section showing arrangement of droop-nose and rear flaps.

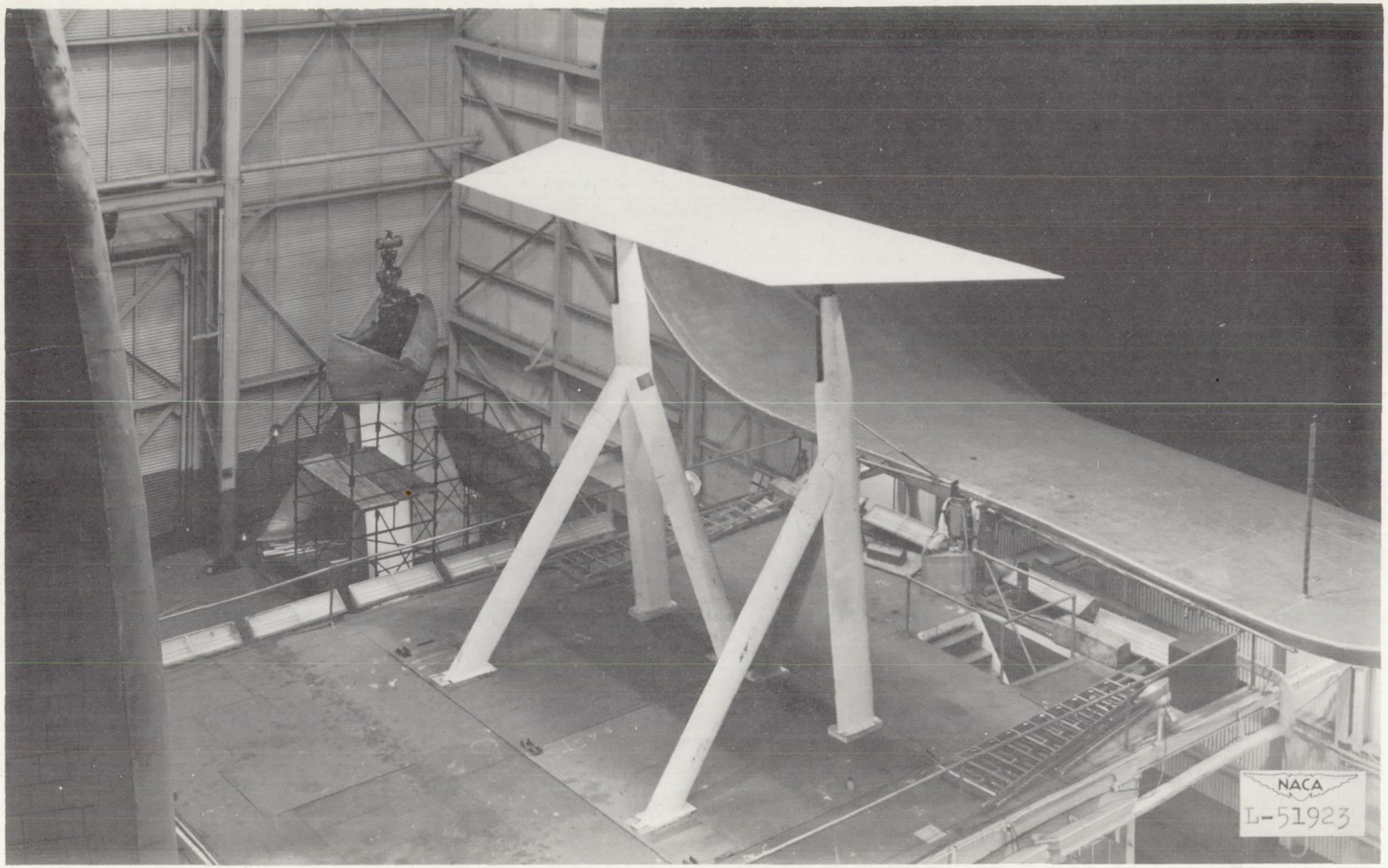

Figure 3.- Three-quarter rear view of wing mounted in the Langley full-scale tunnel. $\delta_f = 0^o$; $\delta_n = 0^o$.

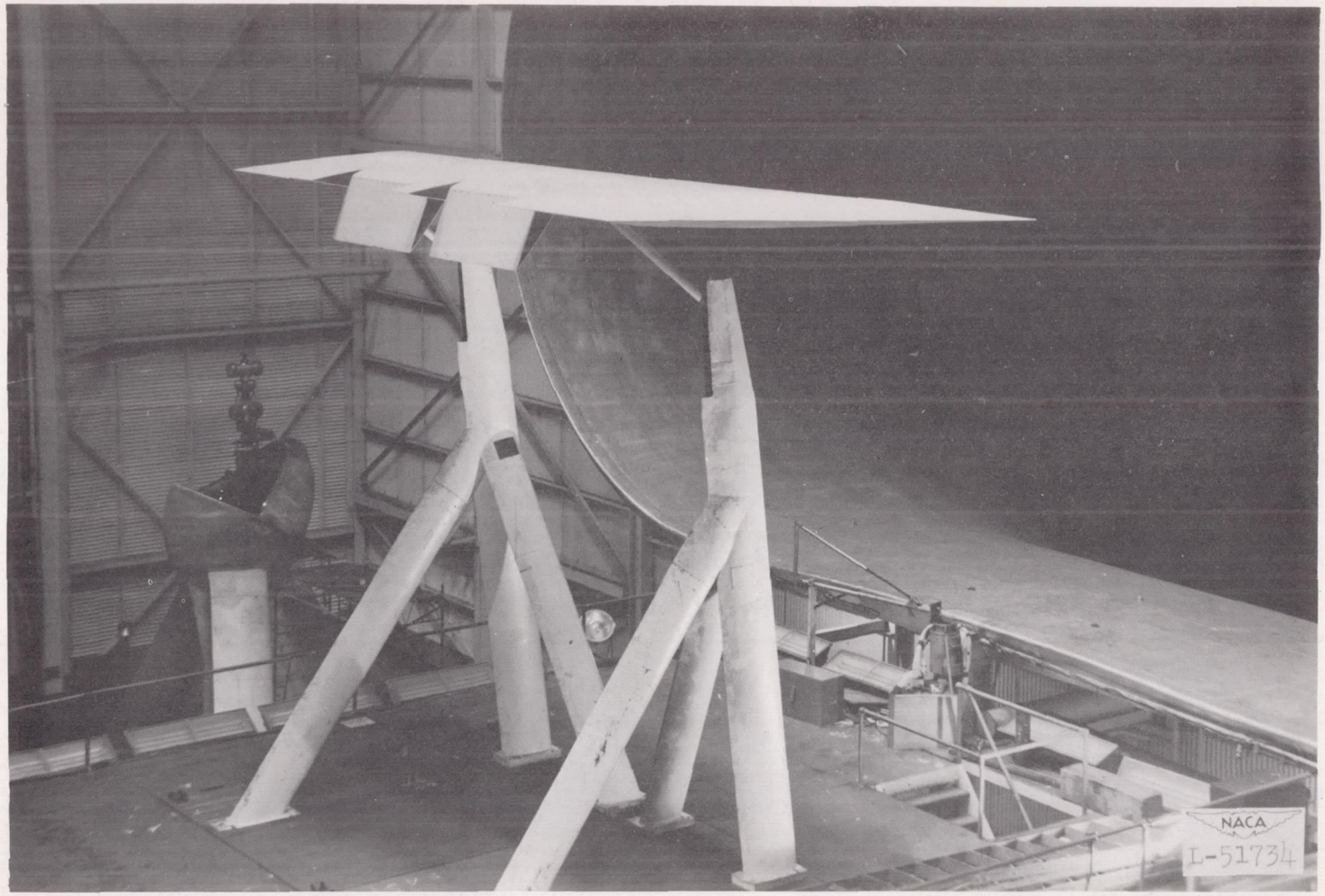

(a) Partial-span rear flaps deflected 60°.

Figure 4.- General views of wing with flaps deflected.

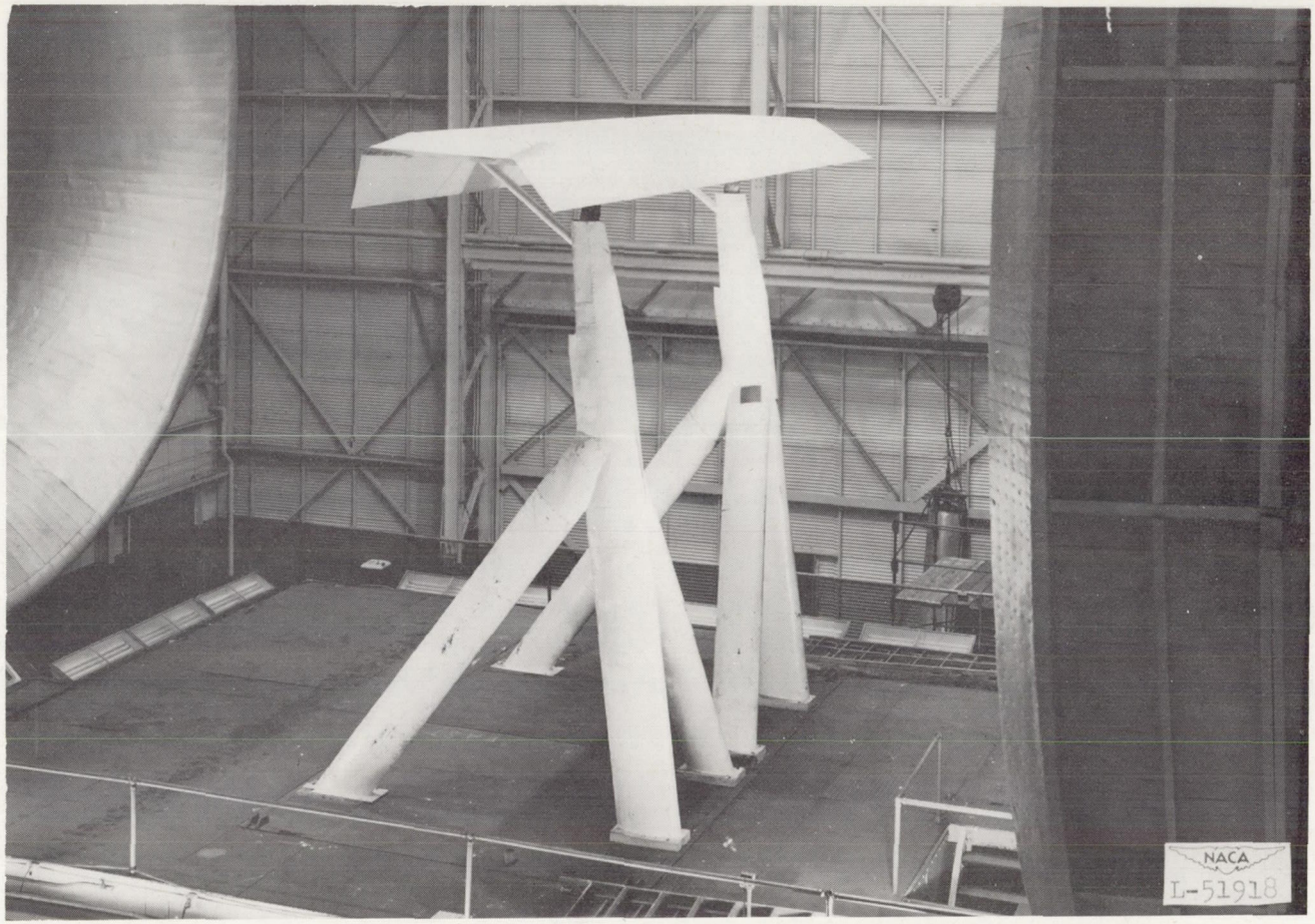

(b) Full-span flaps deflected and droop-nose flaps deflected. $\delta_f = 60^\circ$; $\delta_n = 36^\circ$.

Figure 4.- Concluded.

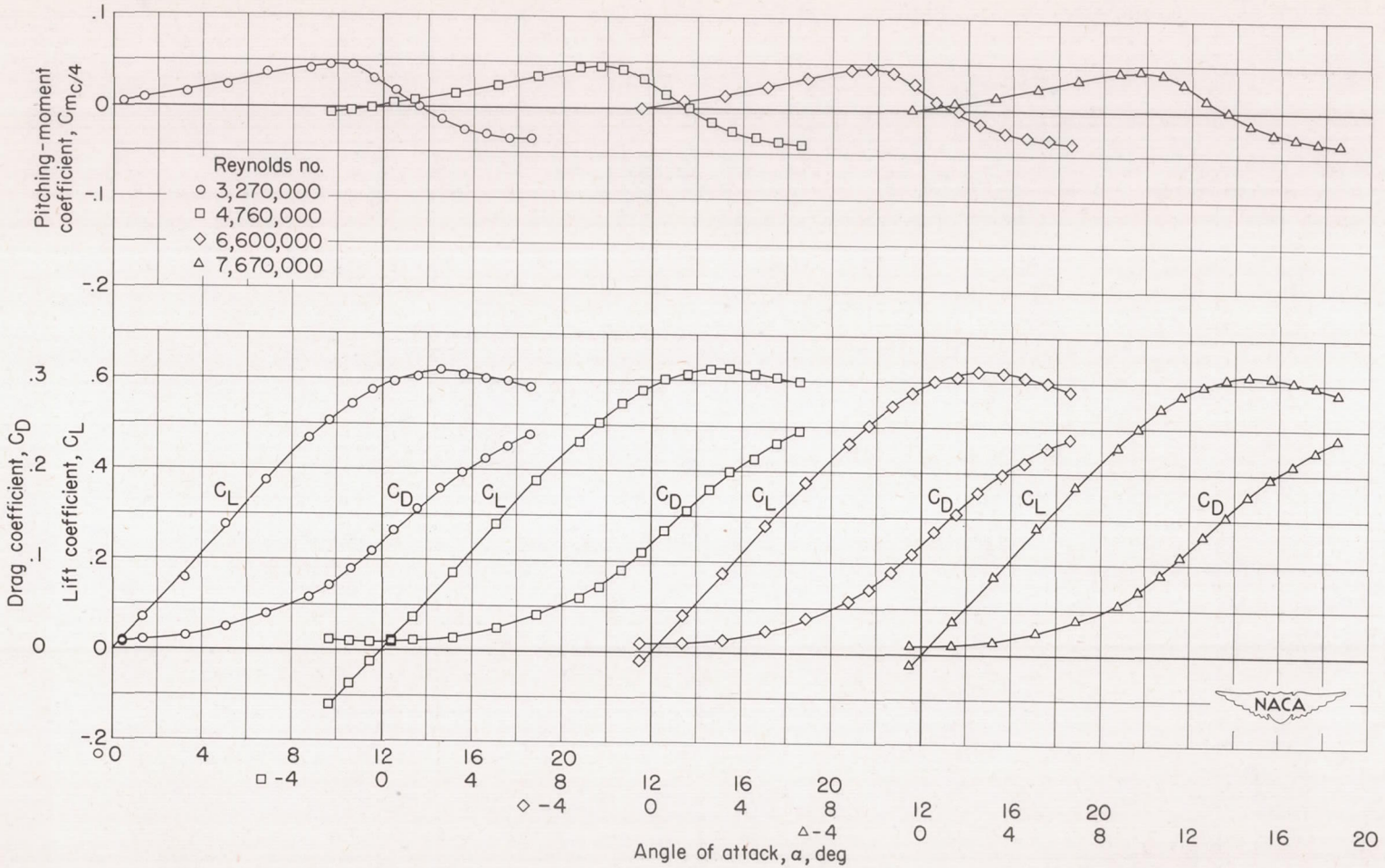

(a) Variation of C_L, C_D, and C_m with α.

Figure 5.- Effect of Reynolds number on the aerodynamic characteristics of a trapezoidal wing. $\delta_f = 0^o$; $\delta_n = 0^o$.

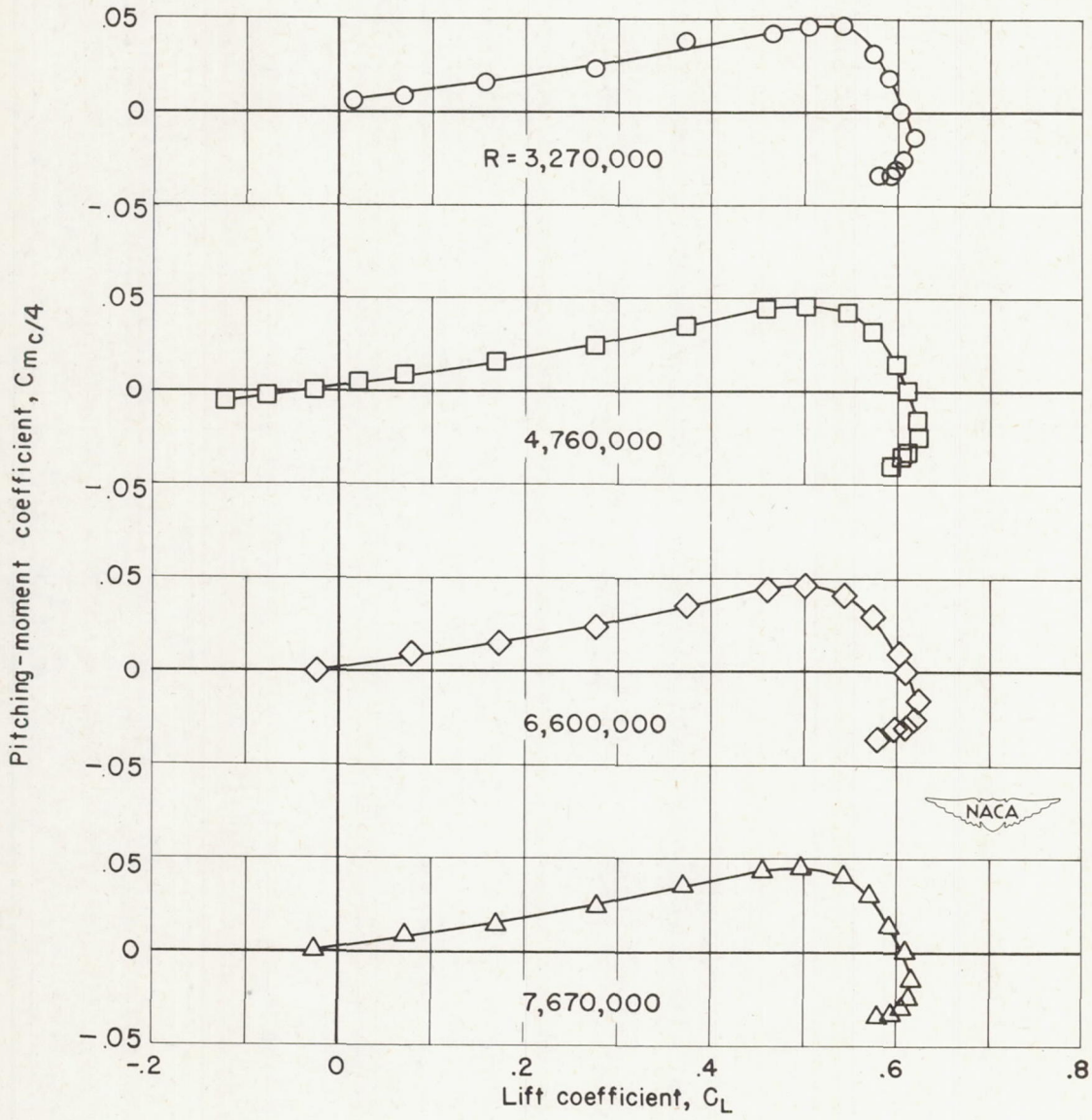

(b) Variation of $C_{m_{c/4}}$ with C_L.

Figure 5.- Concluded.

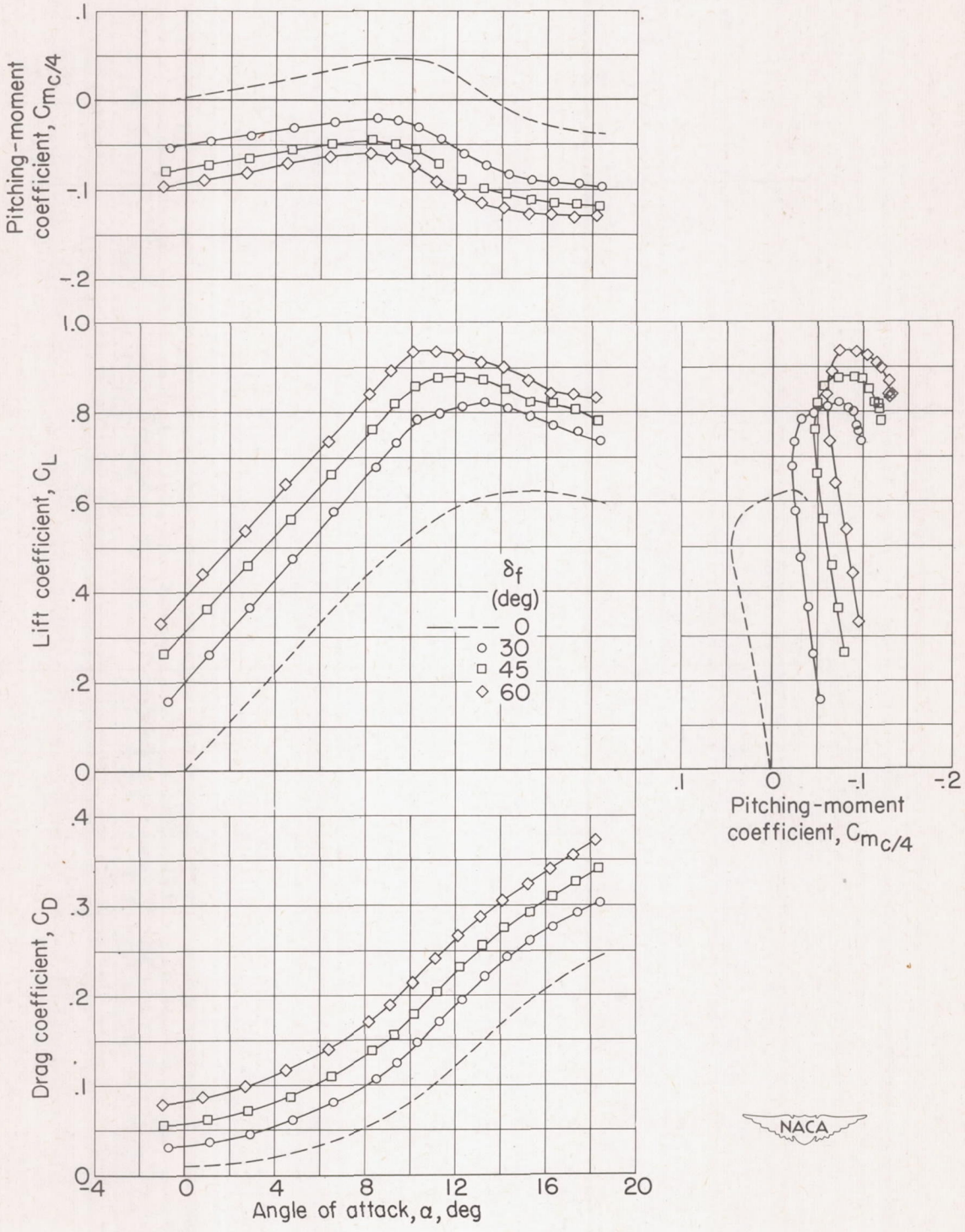

(a) Partial-span flaps.

Figure 6.- Effect of flap deflection on the aerodynamic characteristics of a trapezoidal wing. $\delta_n = 0^o$.

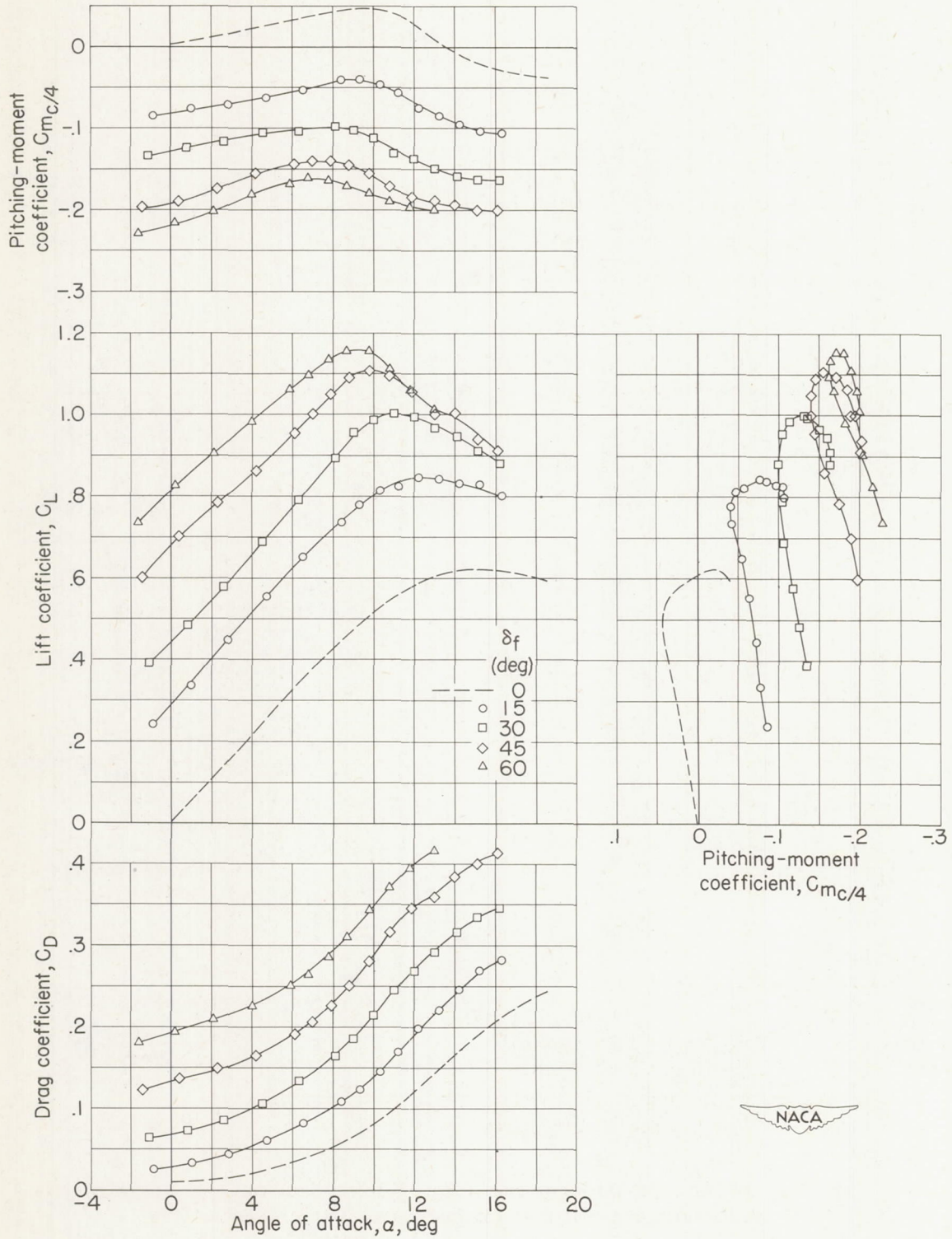

(b) Full-span flaps.

Figure 6.- Concluded.

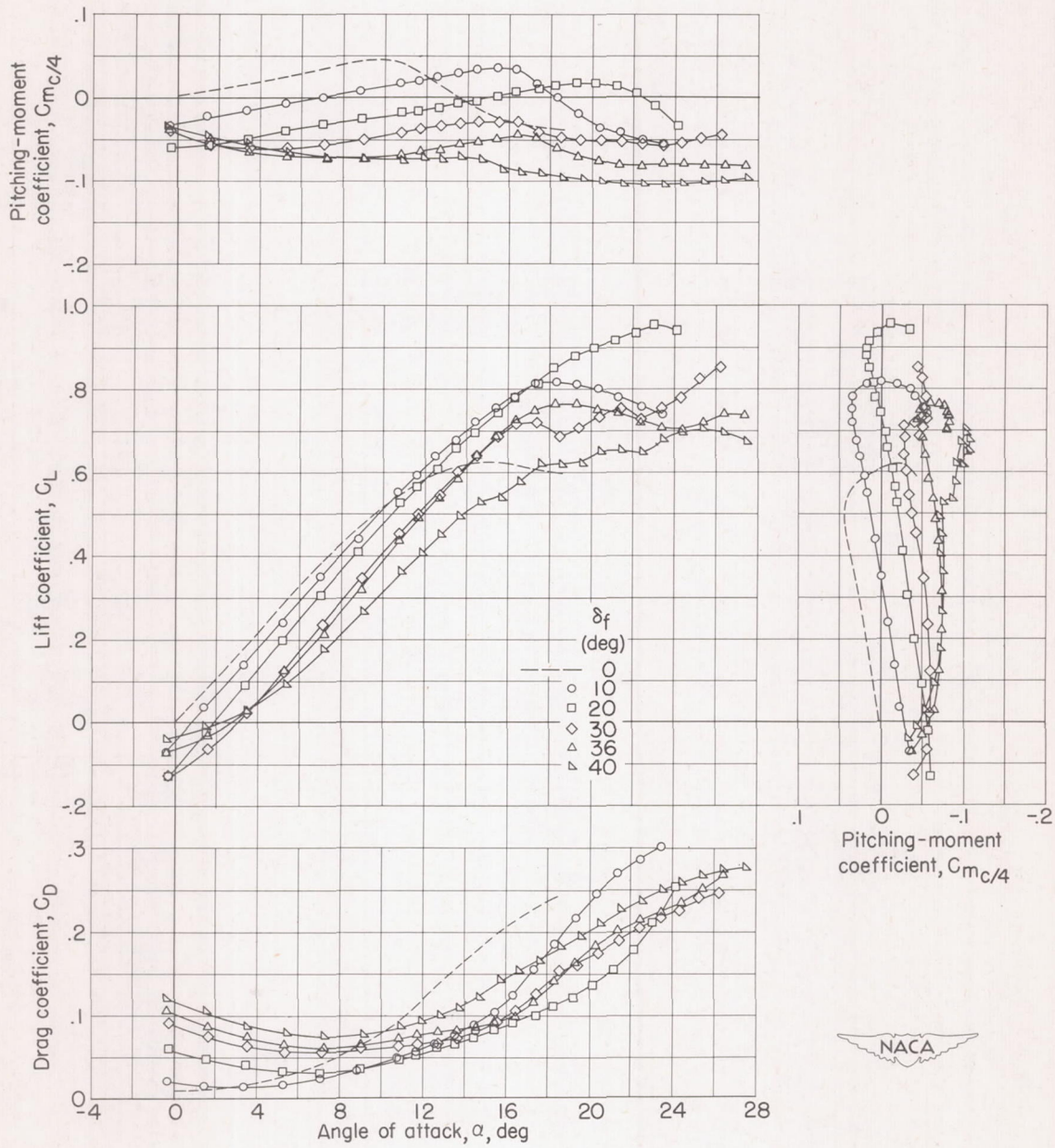

Figure 7.- Effect of droop-nose-flap deflection on the aerodynamic characteristics of a trapezoidal wing. $\delta_f = 0^o$.

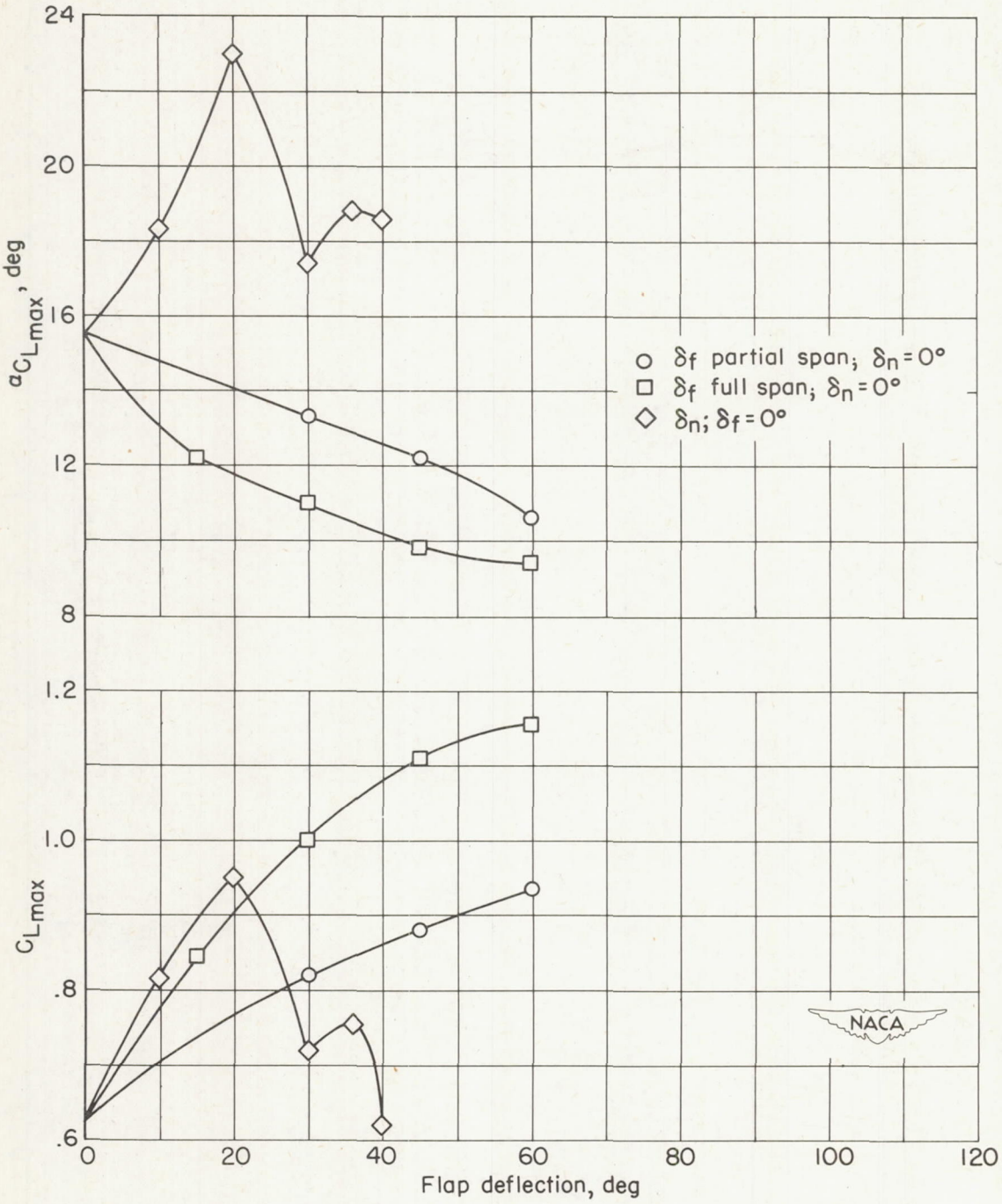

Figure 8.- Summary of maximum lift characteristics as affected by flap deflection.

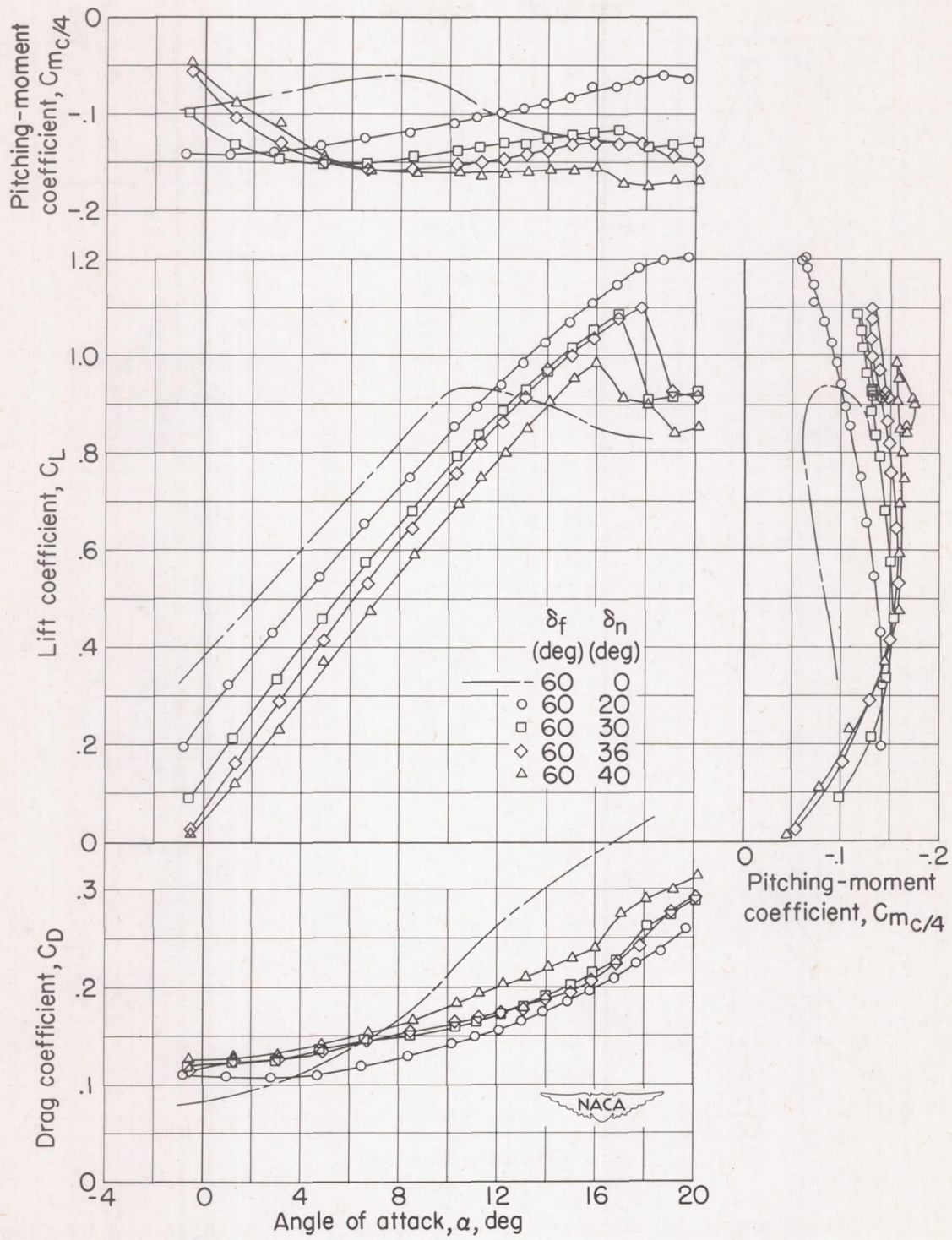

(a) Partial-span rear flaps.

Figure 9.- Aerodynamic characteristics of a trapezoidal wing with combined deflections of flaps.

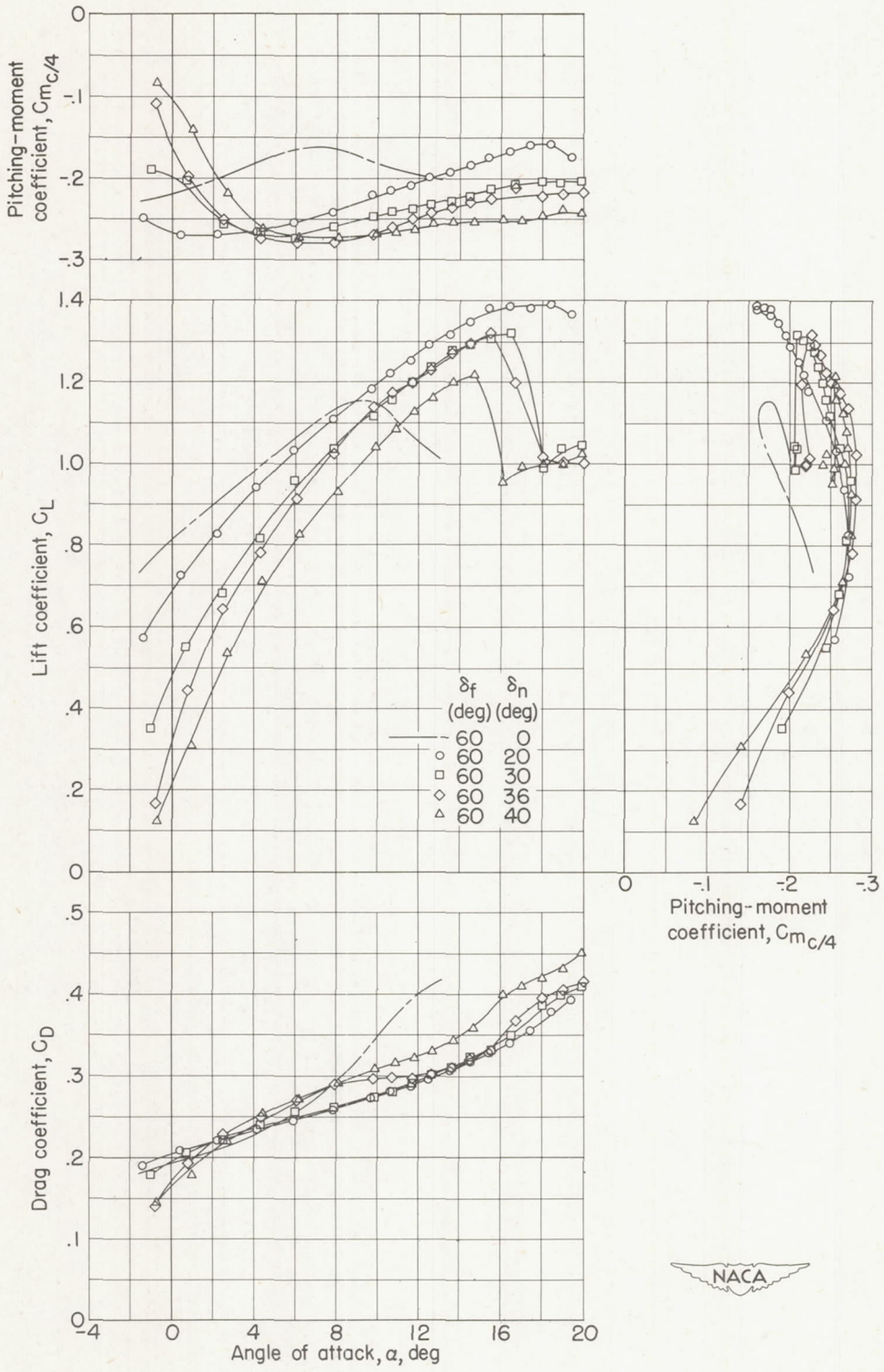

(b) Full-span rear flaps.

Figure 9.- Concluded.

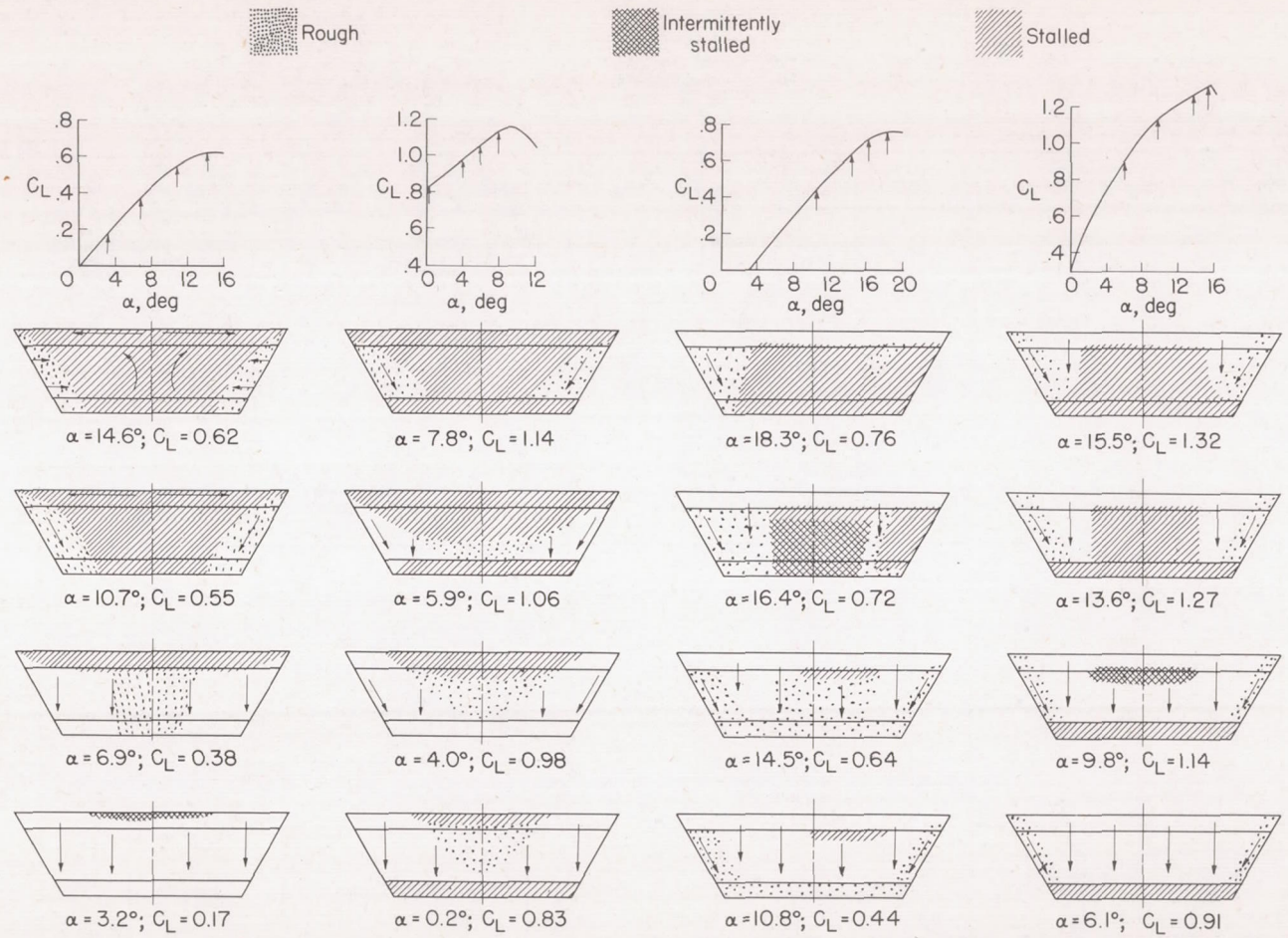

(a) $\delta_f = 0^\circ$; $\delta_n = 0^\circ$. (b) $\delta_f = 60^\circ$; $\delta_n = 0^\circ$. (c) $\delta_f = 0^\circ$; $\delta_n = 36^\circ$. (d) $\delta_f = 60^\circ$; $\delta_n = 36^\circ$.

Figure 10.- Stalling characteristics of a trapezoidal wing with flaps retracted and deflected. Rear flaps are full span. Arrows indicate direction of flow.

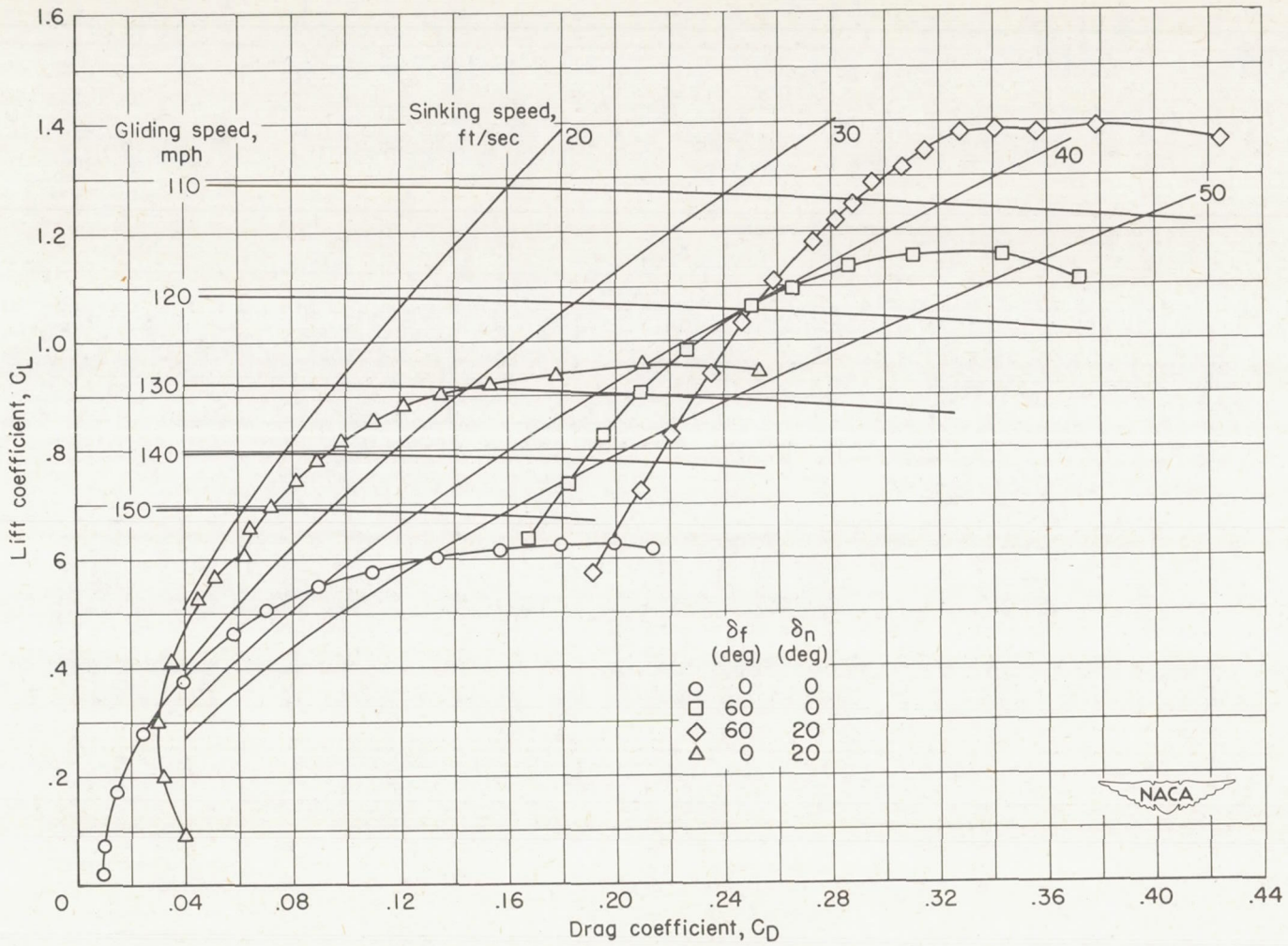

Figure 11.- Landing-approach speeds of basic wing and of wing with full-span-rear and droop-nose flaps deflected. Wing loading, 40 pounds per square foot.

NACA-Langley - 11-13-52 - 1000